The Role of Solvates in Optical Resolution. A Study of the Diastereoisomeric Salts Formed From Enantiomeric 2-Amino-2-phenylethanol and (*R*)-Mandelic Acid, their Crystal Structures and Physico-chemical Properties

Sine Larsen,[*,a] **Dávid Kozma**[a,b] **and Maria Ács**[†,b]
[a] *Department of Chemistry, University of Copenhagen, Universitetsparken 5, DK-2100 Copenhagen, Denmark*
[b] *Department of Organic Chemical Technology, Technical University of Budapest, H-1521 Budapest, POB 91, Hungary*

The reactions between (*R*)-mandelic acid and the pure enantiomers of 2-amino-2-phenylethanol in water saturated ethyl acetate resulted in the diastereoisomeric salts, (*R*)-2-hydroxy-1-phenylethylammonium (*R*)-mandelate hydrate, (*R*-APE)(*R*-MA)·H_2O and (*S*)-2-hydroxy-1-phenylethylammonium (*R*)-mandelate, (*S*-APE)(*R*-MA). Similar reactions from pure ethyl acetate gave the latter salt and unhydrated (*R*-APE)(*R*-MA). The crystal structures at 122 K have been determined for the salts obtained from water-saturated ethyl acetate. The less soluble salt, (*R*-APE)(*R*-MA)·H_2O, crystallizes in *C*2, a = 18.407(2), b = 5.5940(6), c = 15.1863(10) Å, β = 105.735(6)°, Z = 4, R =0.029 based on 2950 observed reflections. (*S*-APE)(*R*-MA) crystallizes in *P*1, a = 10.0046(12), b = 10.2466(11), c = 15.869(2) Å, α = 100.347(10), β = 98.770(10), γ = 108.437(9)°, Z = 4, R =0.033 based on 6085 contributing reflections. Five independent cations and anions are found in different conformations. Hydrogen bonding is important for the crystal packing in both structures. The water molecule in (*R*-APE)(*R*-MA)·H_2O plays an important role linking cations and anions. The solubilities in pure and water saturated ethyl acetate and the thermal behaviour have been investigated for the three compounds (*R*-APE)(*R*-MA)·H_2O, (*R*-APE)(*R*-MA) and (*S*-APE)(*R*-MA). The difference in thermochemical properties can be related to the differences in the crystal packing and explain why the resolution of 2-amino-2-phenylethanol with (*R*)-mandelic acid can only be achieved in water-saturated ethyl acetate.

From the measured solubilities $\Delta G^\ominus$ has been calculated for the reaction: (*R*-APE)(*R*-MA) + $H_2O \longrightarrow$ (*R*-APE)(*R*-MA)·H_2O; $\Delta G^\ominus = -3.4$ kJ mol^{-1}.

Since its inception by Pasteur in 1853, optical resolution *via* diastereoisomeric salt formation has remained one of the most frequently used methods for separating enantiomers of a given racemic acid or base. The method involves the formation of ion pairs and a crystallization step in which the separation takes place. Studies concerning the optical resolutions tend mainly to be concerned with either the production of pure enantiomers on a laboratory scale where economical view points get little attention or an industrial scale of separation of enantiomers, where the parameters influencing the efficiency of separation were identified by experiments and the generalizable features are disregarded. Primarily, the separation of the enantiomers depends on chiral discrimination between the enantiomers and the resolving agent. A second but equally important role is played by the solvent, which may influence the formation of crystal nuclei and may also be included in the crystal lattice of the diastereoisomeric salts.

It is not uncommon that the two diastereoisomeric salts obtained by resolution differ with respect to their content of solvent molecules. The difference in the solubilities that makes separation of the diastereoisomeric salts possible may therefore be related to the difference in the solvent content. We have observed that both the resolution of racemic 2-amino-2-phenylethanol with optically active mandelic acid and the reverse of racemic mandelic acid with optically active 2-amino-2-phenylethanol are strongly dependent on the solvent.[1] The separation of enantiomers can be achieved in water-saturated ethyl acetate, but not in pure ethyl acetate. In order to elucidate the significance of the solvent we have investigated the diastereoisomeric (*R*)-mandelic salts formed with the two enantiomers of 2-amino-2-phenylethanol in pure and water-containing ethyl acetate.

In water-containing ethyl acetate we obtained the salts (*R*)-2-hydroxy-1-phenylethylammonium (*R*)-mandelate hydrate (*R*-APE)(*R*-MA)·H_2O and (*S*)-2-hydroxy-1-phenylethylammonium (*R*)-mandelate (*S*-APE)(*R*-MA). In pure ethyl acetate the latter salt is also obtained and unhydrated (*R*-APE)(*R*-MA). The thermochemical properties of the three compounds have been investigated and the crystal structures determined for the salts for which we could obtain suitable crystals for X-ray diffraction, (*R*-APE)(*R*-MA)·H_2O and (*S*-APE)(*R*-MA).

Experimental

(*R*)-Mandelic acid was purchased from Merck, and the enantiomers of 2-amino-2-phenylethanol from SIGMA.

Water-free ethyl acetate was obtained by distillation of commercial (99% purity) ethyl acetate treated with P_2O_5. The fraction boiling at 77 °C (760 mmHg) was used. The water-saturated ethyl acetate was prepared from pure ethyl acetate prepared as described above. Pure ethyl acetate was shaken at room temperature with an excess of distilled water. Water-saturated ethyl acetate was isolated as the upper phase.

Thermochemical Measurements.—These were performed for the three diastereoisomeric salts (*R*-APE)(*R*-MA)·H_2O, (*R*-

---

† Deceased.

APE)(*R*-MA) and (*S*-APE)(*R*-MA). Differential scanning calorimetry (DSC) curves were recorded and integrated with a Polymer Laboratories PL DSC system, samples of 3–4 mg were run under nitrogen atmosphere with a heating rate of 5 °C $\min^{-1}$. The temperature range of thermal decomposition was determined by thermogravimetric measurements performed with a PL TGA 1000 instrument.

The solubilities were measured at 21 ± 0.5 °C. Samples (0.5–1.5 g) were shaken in solvent (100 g) for 24 h. The residue was removed by filtering. Three portions (20 cm^3) were taken from the mother liquor, and gravimetric methods were used to determine the solubility. The values obtained from the three independent experiments were within 5% of their average.

Preparation of the Diastereoisomeric Salts.—(*R*)-Mandelic acid (0.304 g) was dissolved in water-free ethyl acetate (10 cm^3). It was mixed with either (*R*)- or (*S*)-2-amino-2-phenylethanol (0.274 g). By evaporation of the solvent the two diastereoisomeric salts (*R*-APE)(*R*-MA) and (*S*-APE)(*R*-MA) were obtained. Identical reactions were carried out in water-saturated ethyl acetate. The salts obtained were (*R*-APE)(*R*-MA)·H_2O, and (*S*-APE)(*R*-MA). The salts were characterized by DSC and elemental analysis.

The crystals used for the diffraction study of (*R*-APE)(*R*-MA)·H_2O and (*S*-APE)(*R*-MA) were obtained by recrystallization from water-saturated ethyl acetate.

X-Ray Crystallography.—The less soluble salt from water-containing ethyl acetate was found to be the monohydrate (*R*)-2-hydroxy-1-phenylammonium (*R*)-mandelate hydrate (*R*-APE)(*R*-MA)·H_2O, which forms white, plate-like crystals. The more soluble salt (*S*)-2-hydroxy-1-phenylammonium (*R*)-mandelate (*S*-APE)(*R*-MA) crystallizes as prisms. X-Ray diffraction data for both compounds were measured with an Enraf–Nonius CAD-4 diffractometer using graphite monochromatized CuKα radiation. The crystals were cooled to 122 K by an Enraf–Nonius gas-flow low temperature device. The temperature was monitored by a thermocouple placed a few cm above the crystal in the exhaust pipe. The cell dimensions were determined from 22 reflections ($39 < \theta < 47°$) and 20 reflections ($34 < \theta < 43°$) for the (*R*-APE)(*R*-MA)·H_2O and (*S*-APE)(*R*-MA) salts, respectively. The intensities of three standard reflections were recorded every 10 000 s and the orientation of the crystals was checked every 300 reflections. These measurements showed that no mis-setting or deterioration of the crystals had occurred during the data collection. The crystal data and a summary of data collection and structure refinement results are listed in Table 1. Data reduction included corrections for background, Lorentz and polarization effects and reflections related by the symmetry of the crystal class were averaged. Both structures were solved by direct methods using SHELXS86[2] and refined by full matrix least squares minimizing $\Sigma w(|F_o| - |F_c|)^2$.

The absolute configuration of the structures were selected to give the mandelate ions the correct (*R*) absolute configuration. In this connection it can be mentioned that the method devised by Rogers[3] gave the correct absolute configuration to a probability larger than 99.5% in both structures. After anisotropic displacement parameters were introduced, the hydrogen atoms in the structures were shown clearly in a difference density map. The hydrogen atoms that have their position determined by the geometry of the heavier atoms were introduced in idealized positions. The positions of the remaining atoms were taken from the difference density map. The hydrogen atoms were given a fixed isotropic temperature displacement parameter factor of 2.0 $Å^2$. In the (*R*-APE)(*R*-MA)·H_2O salt the positional parameters for the hydrogen atoms were included in the refinement. The contribution from the hydrogen atoms was included in the structure factor calculation, but their parameters were not refined in the (*S*-APE)(*R*-MA) salt.

Table 1 Crystal data and a summary of data collection and structure refinement results

	(*R*-APE)(*R*-MA)·H_2O	(*S*-APE)(*R*-MA)
Formula	$C_{16}H_{21}O_5N$	$C_{16}H_{19}O_4N$
Formula weight/g mol^{-1}	307.35	289.33
[α_D]	−66.6	−34.5
Space group	*C*2	*P*1
T/K	122 ± 1	122 ± 1
λ/Å	CuKα/1.541 84	CuKα/1.541 84
Crystal size/mm	0.05 × 0.15 × 0.40	0.10 × 0.12 × 0.25
Unit cell dimensions		
a/Å	18.407(2)	10.0046(12)
b/Å	5.5940(6)	10.2466(11)
c/Å	15.1863(10)	15.869(2)
α/°	90	100.347(10)
β/°	105.735(6)	98.770(10)
γ/°	90	108.437(9)
V/$Å^3$	1505.1(4)	1479.5(7)
Z	4	4
d_{cal}/g cm^{-3}	1.356	1.299
μ/cm^{-1}	7.95	7.29
θ range/°	1–75	1–75
Octants measured	$h \pm k \pm l$	$h \pm k \pm l$
Number of unique reflections	3106	6543
Number of contributing reflections	2950	6085
$(\|F\|^2) > P\sigma(\|F\|)^2$		
P	2	1
Weights, w^{-1}	$\sigma^2_{cs}(F) + 0.0009\|F\|^2$	$\sigma^2_{cs}(F) + 0.0006\|F\|^2$
Number of variables, *m*	261	757
R(*F*)	0.029	0.033
$R_w(F)$	0.039	0.041
$S = \left\{\frac{\Sigma w \Delta F^2}{(n-m)}\right\}^{\frac{1}{2}}$	1.13	1.24
Max shift/error in final cycle	0.22	0.07
Min and max peak in $\Delta\rho$/e $Å^{-3}$	−0.37, 0.37	−0.29, 0.29

The SDP system[4] was used for the crystallographic computations. The atomic scattering factors including contribution from anomalous scattering were taken from International Tables for X-Ray Crystallography.[5]

The final positional parameters, anisotropic displacement parameters, parameters for the hydrogen atoms and lists of observed and calculated structure amplitudes have been deposited.*

Results and Discussion

Description of the Structures.—2-Hydroxy-1-phenylethylammonium ions and (*R*)-mandelate ions are found in both diastereoisomeric salts. The asymmetric unit (unit cell) of the more soluble (*S*-APE)(*R*-MA) salt contains four cations and anions, so this investigation provides structural information for five independent 2-hydroxy-1-phenylethylammonium ions and five independent (*R*)-mandelate anions.

The bond lengths, bond and torsion angles of the cations as observed in the two structures are listed in Table 2. The molecular dimensions of the five cations agree very well internally. This cation has not been described in other crystal

---

* For details of the deposition scheme see 'Instructions for Authors (1994),' *J. Chem. Soc., Perkin Trans. 2*, Issue 1, 1994.

Table 2 Molecular geometry of the 2-hydroxy-1-phenylethylammonium ions. Bond lengths in Å, bond and torsion angles in deg.

	R-APE	*S*-APE			
	Label A	Label A	Label B	Label D	Label E
C(1)–C(2)	1.529(2)	1.516(7)	1.523(6)	1.520(7)	1.523(7)
C(1)–O	1.4200(13)	1.420(6)	1.409(6)	1.417(6)	1.404(7)
C(2)–C(3)	1.5168(14)	1.523(7)	1.515(7)	1.516(7)	1.516(7)
C(2)–N	1.4978(14)	1.508(6)	1.491(6)	1.489(6)	1.496(6)
C(3)–C(4)	1.392(2)	1.393(7)	1.397(7)	1.389(7)	1.389(7)
C(3)–C(8)	1.392(2)	1.390(7)	1.392(7)	1.397(7)	1.390(7)
C(4)–C(5)	1.394(2)	1.382(8)	1.394(7)	1.390(8)	1.390(8)
C(5)–C(6)	1.385(2)	1.384(9)	1.379(8)	1.379(9)	1.381(10)
C(6)–C(7)	1.387(2)	1.382(8)	1.383(8)	1.389(9)	1.379(9)
C(7)–C(8)	1.395(2)	1.388(8)	1.396(8)	1.386(8)	1.399(8)
C(2)–C(1)–O	112.21(9)	108.9(4)	107.6(4)	108.9(4)	109.1(4)
C(1)–C(2)–N	108.26(9)	109.3(4)	107.5(4)	109.4(4)	109.2(4)
C(1)–C(2)–C(3)	111.60(9)	113.2(4)	112.7(4)	109.6(4)	113.1(4)
N–C(2)–C(3)	111.28(9)	111.2(4)	111.9(4)	112.1(4)	111.7(4)
C(2)–C(3)–C(4)	119.67(10)	119.8(5)	117.6(4)	120.3(5)	118.5(5)
C(2)–C(3)–C(8)	121.42(10)	120.9(4)	123.4(5)	120.5(5)	122.0(5)
O–C(1)–C(2)–N	−61.01(12)	64.2(2)	−61.2(2)	52.3(2)	−57.8(2)
O–C(1)–C(2)–C(3)	176.19(9)	−171.3(2)	62.6(2)	175.5(2)	67.3(2)
C(1)–C(2)–C(3)–C(4)	−102.09(13)	150.7(2)	87.1(2)	111.1(2)	102.3(2)
C(1)–C(2)–C(3)–C(8)	76.46(14)	−26.6(3)	−91.1(2)	−64.1(3)	−74.7(3)
N–C(2)–C(3)–C(8)	−44.6(2)	96.9(2)	30.2(3)	57.6(3)	49.0(3)
N–C(2)–C(3)–C(4)	136.85(11)	−85.8(3)	−151.7(2)	−127.3(2)	−134.0(2)

structures listed in the Cambridge Structural Database, only amides of this amine have previously been studied structurally.[7,8] As it is apparent from Fig. 1 as well as the torsion angles listed in Table 2, the ions exhibit great variation in their conformation. This may be a consequence of the presence of two functional groups, as distinctly favoured conformations are found for the related 1-phenylethylammonium cation.[9] The O–C(1)–C(2)–N fragment adopts a gauche conformation in all five cations with torsion angles close to ± 60°, but the remaining part of the cation seems to be very flexible. The orientation of the phenyl group is similar in cations D and E in the more soluble (*S*-APE)(*R*-MA) salt, resembling the mirror image of the cation in the less soluble salt. A comparison of the torsion angles listed in Table 2 reveals that the torsion angles of cation D do not differ more than 13° from those of the mirror image of the cation in the less soluble salt. The orientation of the phenyl group in the cations A and B are twisted *ca.* 40–50° relative to the orientation in C and D.

Equivalent observations can be made for the (*R*)-mandelate ions. The bond lengths and angles of the five mandelate ion listed in Table 3 are virtually identical and compare well with the molecular dimensions found in other mandelate salts.[10] The conformation of the mandelate ion can conveniently be described by the torsion angles O(1)–C(1)–C(2)–O(3) and O(3)–C(2)–C(3)–C(4). In a recent analysis of the stereochemistry of mandelate salts[10] we found that the torsion angle O(1)–C(1)–C(2)–O(3) was in the range − 10 to 40°.

The different O(1)–C(1)–C(2)–O(3) torsion angles listed in Table 3 all fall into this range. The anions labelled X and Z in (*S*-APE)(*R*-MA) have an almost planar arrangement of the O(1)–C(1)–C(2)–O(3) moiety, only in the Z anion can this be explained by the presence of an intramolecular hydrogen bond (Fig. 2).

The relative orientation of the phenyl group described by the torsion angles O(3)–C(2)–C(3)–C(4) or C(1)–C(2)–C(3)–C(4) display much larger variations. In most mandelate salts the value for this angle is found in the range 90 to 180°. The mandelate ions in the more soluble salt fit well into this pattern, but it should be noted that mandelate ion in (*R*-APE)(*R*-MA)·H_2O does not conform to this common picture. The different conformation of the mandelate ion in this compound seems to be due to intermolecular interactions between the phenyl groups (*vide infra*).

Crystal Packing.—The significant variations in the conformations of the cations and anions are caused by intermolecular interactions in the crystals, which are strongly dominated by hydrogen bonding in both structures. The hydrated (*R*-APE)-(*R*-MA)·H_2O contains seven protons that could be expected to take part in hydrogen bonding and five possible acceptor atoms. As shown in Table 4 all protons are involved in hydrogen bonds. The positively charged ammonium group is hydrogen bonded to three mandelate ions, it denotes protons to two carboxylate and one hydroxy group. The OH group of the cation accepts a proton from yet another mandelate ion to make each cation interacting with four different anions through hydrogen bonds. The water molecule donates protons to the OH- and the COO- group from two different mandelate ions and accepts the proton from the OH group of a cation. From these interactions it is obvious that the water molecule plays an important and integral part of the crystal packing connecting the cations and anions.

The stereo pair in Fig. 3 illustrates how this network of hydrogen bonds connects the water molecule and the hydrophilic parts of the ions to form layers parallel to the *a–b* plane, and the weaker interactions between the almost parallel phenyl groups in the direction of the *c*-axis in accordance with the plate-like growth of the crystals.

In the more soluble (*S*-APE)(*R*-MA) salt the crystal packing is also strongly dominated by the hydrogen bonding as shown in Table 5. Cation A is interacting with five mandelate ions donating protons to four and accepting one from anion X. The cations labelled B, D and E are all hydrogen bonded to four different mandelate ions so in this sense there is a strong resemblance to the environment of the cation in the less soluble (*R*-APE)(*R*-MA)·H_2O salt. However, the interactions of the anions are different in the two salts. In the anion labelled Z an intramolecular hydrogen bond is formed between the OH- and the COO- groups. The hydroxy group of anion X donates a proton to cation A. O(1) of the carboxylate group in X accepts the protons from the OH groups of anions W and Y. This complex network of hydrogen bonds in the more soluble (*S*-APE)(*R*-MA) salt is illustrated on the stereo pair in Fig. 4.

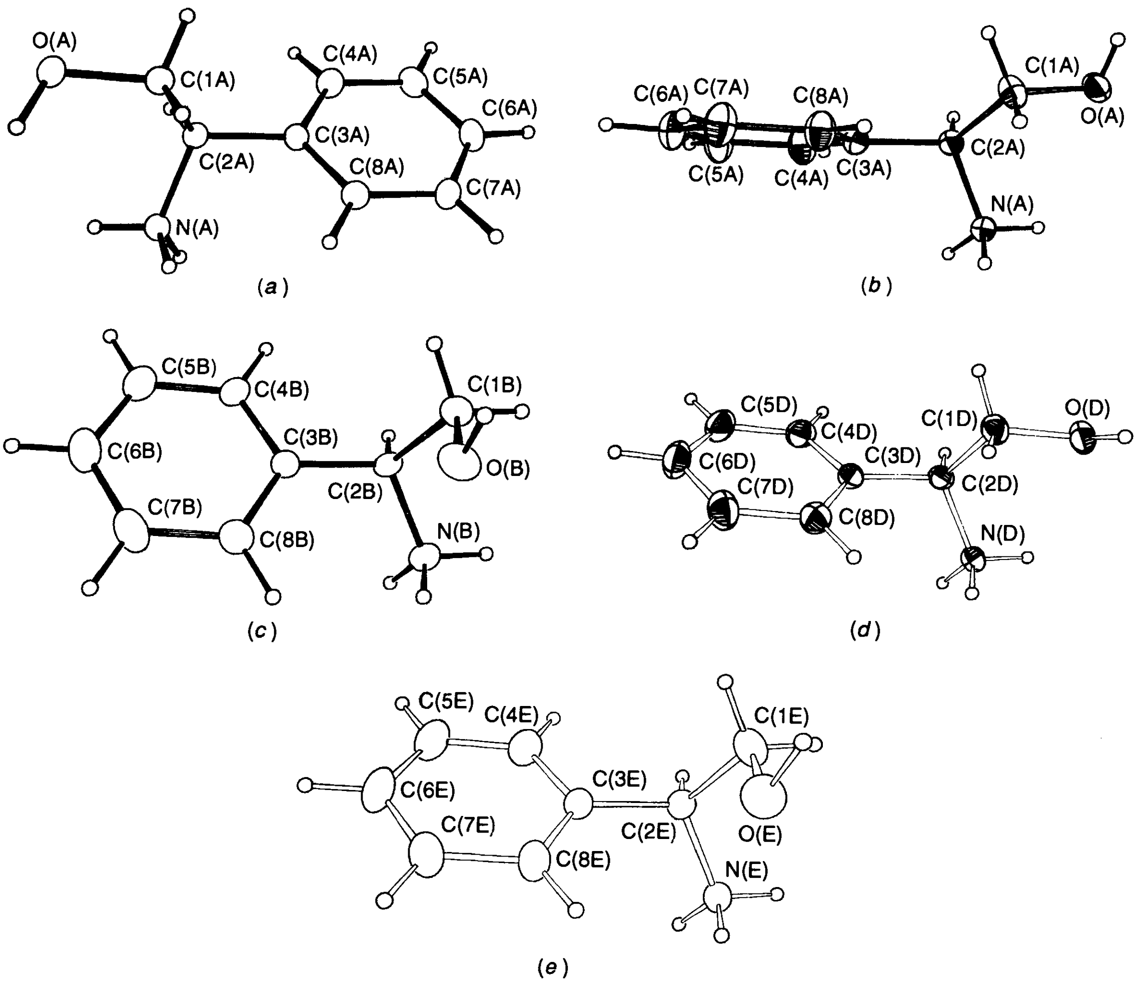

Fig. 1 ORTEP drawings illustrating the stereochemistry and the atomic numbering scheme of the enantiomers 2-hydroxy-1-phenylammonium ions as observed in (*a*) (*R*-APE)(*R*-MA)·H_2O and in (*S*-APE)(*R*-MA) (*b*) (*c*) (*d*) and (*e*). The thermal ellipsoids are scaled to enclose 50% probability, the hydrogen atoms are drawn as spheres with a fixed radius.

Table 3 Molecular geometry of the (*R*)-mandelate ions. Bond lengths in Å, bond and torsion angles in deg.

	(*R*-APE)(*R*-MA)·H_2O	(*S*-APE)(*R*-MA)			
	Label X	Label W	Label X	Label Y	Label Z
C(1)–O(1)	1.266(2)	1.251(6)	1.260(6)	1.245(6)	1.257(6)
C(1)–O(2)	1.254(2)	1.259(6)	1.255(6)	1.270(6)	1.254(6)
C(1)–C(2)	1.533(2)	1.536(7)	1.535(7)	1.538(7)	1.543(7)
C(2)–O(3)	1.436(13)	1.428(6)	1.426(6)	1.426(6)	1.423(6)
C(2)–C(3)	1.521(2)	1.520(7)	1.514(7)	1.506(7)	1.520(7)
C(3)–C(4)	1.394(2)	1.394(7)	1.392(7)	1.391(7)	1.394(7)
C(3)–C(8)	1.394(2)	1.393(7)	1.392(7)	1.394(7)	1.390(7)
C(4)–C(5)	1.391(2)	1.392(8)	1.387(8)	1.393(8)	1.388(9)
C(5)–C(6)	1.390(2)	1.384(9)	1.380(8)	1.386(8)	1.381(10)
C(6)–C(7)	1.389(2)	1.383(8)	1.391(8)	1.391(8)	1.383(9)
C(7)–C(8)	1.399(2)	1.394(7)	1.390(8)	1.394(8)	1.386(8)
O(1)–C(1)–O(2)	124.72(11)	124.2(5)	125.0(4)	125.5(5)	125.9(5)
O(1)–C(1)–C(2)	118.75(10)	117.7(4)	119.2(4)	119.3(4)	115.3(4)
O(2)–C(1)–C(2)	116.50(10)	118.2(4)	115.8(4)	115.2(4)	118.8(4)
O(3)–C(2)–C(1)	112.68(9)	107.5(4)	112.0(4)	112.4(4)	108.7(4)
O(3)–C(2)–C(3)	110.56(9)	112.9(4)	107.6(4)	110.1(4)	111.1(4)
C(1)–C(2)–C(3)	111.89(9)	108.3(4)	112.1(4)	107.9(4)	110.4(4)
C(2)–C(3)–C(4)	118.40(10)	120.5(5)	120.8(5)	119.3(5)	120.6(5)
C(2)–C(3)–C(8)	122.11(10)	120.5(4)	119.9(4)	121.4(5)	120.4(5)
O(1)–C(1)–C(2)–O(3)	25.15(13)	37.8(2)	−8.0(3)	29.4(2)	3.0(2)
O(1)–C(1)–C(2)–C(3)	−100.16(11)	−84.5(2)	−129.1(2)	−92.3(2)	−119.2(2)
C(1)–C(2)–C(3)–C(4)	−164.38(10)	−77.1(3)	−128.5(2)	−92.8(2)	−94.1(3)
C(1)–C(2)–C(3)–C(8)	18.62(15)	100.6(2)	53.5(3)	84.7(3)	84.2(3)
O(3)–C(2)–C(3)–C(4)	69.15(13)	164.0(2)	107.9(2)	144.1(2)	145.2(2)
O(3)–C(2)–C(3)–C(8)	−107.85(12)	−18.4(3)	−70.2(2)	−38.4(2)	−36.5(3)

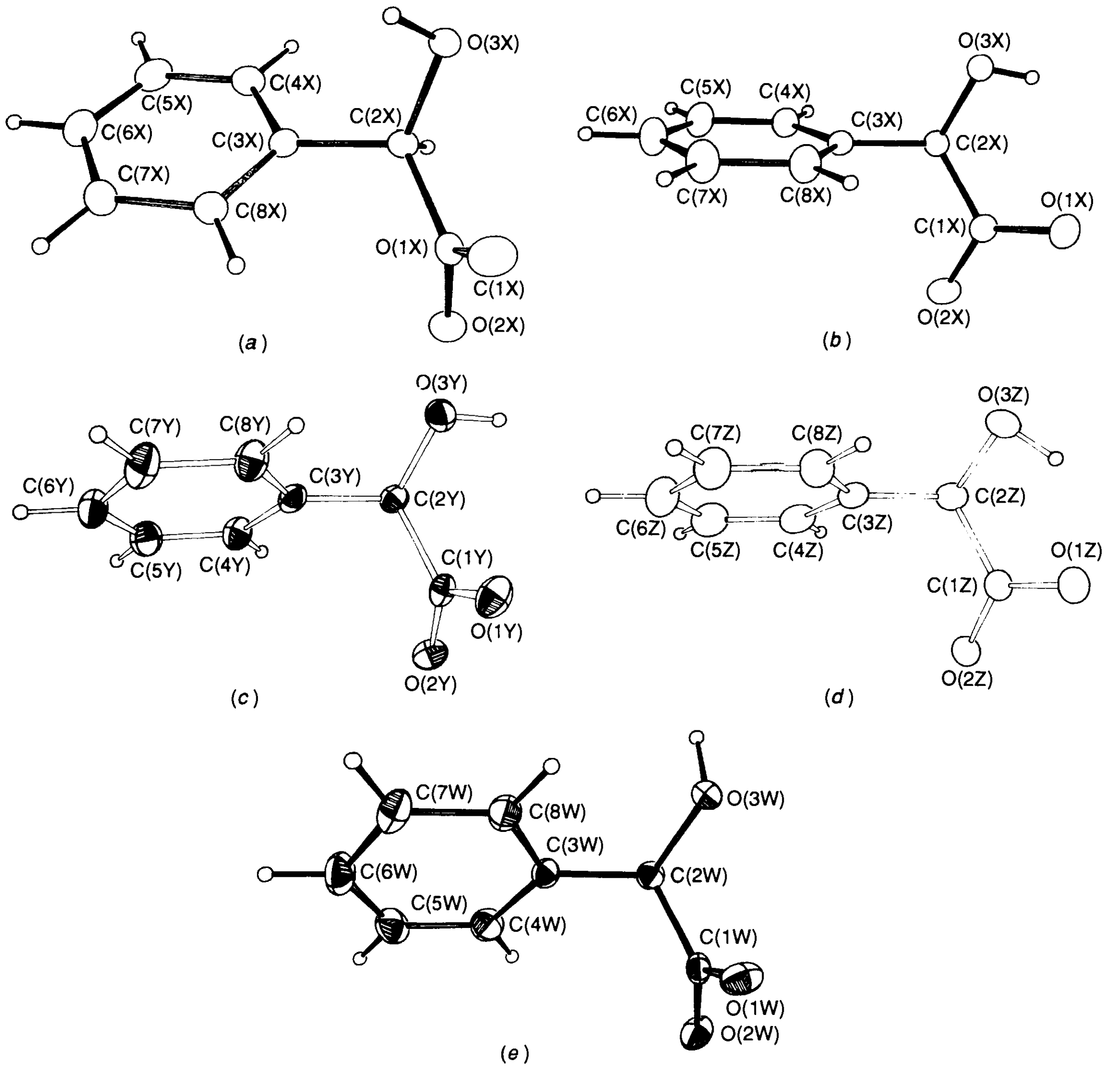

Fig. 2 ORTEP drawings of the five independent (*R*)-mandelate ions observed in (*R*-APE)(*R*-MA)·H_2O (*a*) and in (*S*-APE)(*R*-MA) (*b*, *c*, *d* and *e*). The anions are drawn as the cations (Fig. 1).

Table 4 Hydrogen bonds in the (*R*)-2-hydroxy-1-phenylethylammonium (*R*)-mandelate hydrate

D–H ··· A	D ··· A/Å	D–H ··· A/°	H ··· A/Å
O(A)–H(A)–O(W)	2.6460(13)	171(2)	1.73(2)
N(A)–HN(A1)–O(1X)[a]	2.8188(13)	169(2)	1.84(2)
N(A)–HN(A2)–O(3X)[b]	2.8749(12)	163(2)	1.98(2)
N(A)–HN(A3)–O(2X)[c]	2.8074(14)	176(2)	1.86(2)
O(3X)–HO(3X)–O(A)	2.7061(12)	173(2)	1.93(2)
O(W)–HO(W1)–O(1X)[b]	2.7717(14)	176(2)	1.84(2)
O(W)–HO(W2)–O(3X)[d]	2.8249(12)	160(2)	1.96(2)

[a] $(x - \frac{1}{2}, \frac{1}{2} + y, z)$. [b] $(1 - x, y, 1 - z)$. [c] $(x - \frac{1}{2}, y - \frac{1}{2}, z)$. [d] $(1 - x, y - 1, 1 - z)$.

Thermodynamic Stability and Its Relation to the Crystal Structures.—In the preparation of the diastereoisomeric salts from (*R*)-mandelic acid and the enantiomers from 2-amino-2-phenylethanol we were able to isolate two different salts that contain the (*R*)-enantiomer of the base. In water-saturated ethyl acetate we obtained a hydrate whereas the equivalent water-free salt precipitated from pure ethyl acetate. The existence of different (*R*-APE)(*R*-MA) salts may explain why the resolution of the racemic 2-amino-2-phenylethanol can only be achieved in water-containing ethyl acetate.

Table 5 Hydrogen bonds in (*S*)-2-hydroxy-1-phenylethylammonium (*R*)-mandelate

D–H ··· A	D ··· A/Å	D–H ··· A/°	H ··· A/Å
O(A)–HO(A)–O(2Z)	2.648(5)	165	1.88
N(A)–HN(A1)–O(2Y)[a]	2.676(5)	139	1.88
N(A)–HN(A2)–O(3W)[b]	2.967(5)	132	2.25
N(A)–HN(A3)–O(3Z)[b]	2.845(5)	153	1.96
O(B)–HO(B)–O(2W)	2.691(5)	154	1.97
N(B)–HN(B1)–O(1Y)[a]	2.811(5)	151	1.94
N(B)–HN(B2)–O(2X)[e]	2.772(5)	150	1.90
N(B)–HN(B3)–O(2W)[d]	2.755(5)	153	1.87
O(D)–HO(D)–O(3X)	2.808(5)	173	1.77
N(D)–HN(D1)–O(2X)[d]	2.695(5)	165	1.76
N(D)–HN(D2)–O(1Z)	2.766(5)	163	1.84
N(D)–HN(D3)–O(1W)[c]	2.771(5)	139	1.98
O(E)–HO(E)–O(3Y)[b]	2.782(5)	142	2.00
N(E)–HN(E1)–O(2Y)	2.781(5)	150	1.92
N(E)–HN(E2)–O(2W)[c]	2.818(5)	159	1.91
N(E)–HN(E3)–O(2Z)	2.898(6)	156	2.00
O(3W)–HO(3W)–O(1X)[d]	2.744(5)	166	1.77
O(3X)–HO(3X)–O(A)	2.776(5)	144	2.12
O(3Y)–HO(3Y)–O(1X)[d]	2.975(5)	142	2.24
O(3Z)–HO(3Z)–O(1Z)	2.547(5)	133	1.80

[a] $(1 + x, 1 + y, z)$. [b] $(x, 1 + y, z)$. [c] $(x - 1, y, z)$. [d] $(x, y - 1, z)$. [e] $(1 + x, y, z)$.

Table 6 Thermodynamic data for the diastereoisomeric salts

	(R-APE)(R-MA)·H_2O	(R-APE)(R-MA)	(S-APE)(R-MA)
Melting point, T_f/°C	141(1)	137(1)	119(1)
Dehydration temp. (loss of water)	55–85	—	—
$\Delta H_f^{\theta us}(T_f)$/kJ mol^{-1}	(34)	27(2)	30(2)
$\Delta S_f^{\theta us}(T_f)$/J K^{-1} mol^{-1}	(82)	66(5)	76(5)
Solubilities at 21 °C/mol (kg solvent)$^{-1}$:			
pure ethyl acetate (ea)	—	0.0039(2)	0.0076(3)
water-saturated ethyl acetate (ew)	0.0104(3)	—	0.0404(4)

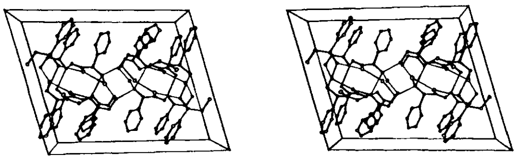

Fig. 3 Stereo pair illustrating the packing in (R)-2-hydroxy-1-phenylethylammonium (R)-mandelate hydrate. The hydrogen bonds are drawn as thin lines.

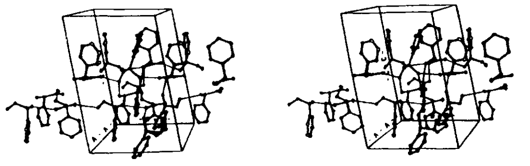

Fig. 4 Stero pair illustrating the packing in (S)-2-hydroxy-1-phenylammonium (R)-mandelate. To distinguish the four independent cations and anions they are drawn in the same way as in Fig. 1 and Fig. 2. Hydrogen bonds are shown as thin lines.

In order to investigate if this difference is of thermodynamic or kinetic origin, the solubilities were determined for the diastereoisomeric salts (R-APE)(R-MA)·H_2O and (S-APE)(R-MA) in water-saturated ethyl acetate and for (R-APE)(R-MA) and (S-APE)(R-MA) in water-free ethyl acetate. The solubilities are presented in Table 6 along with the results from the DSC measurements. These results show that the solubilities are larger in water-saturated ethyl acetate. In this solvent (S-APE)(R-MA) is *ca.* four times more soluble than the other diastereoisomeric salt (R-APE)(R-MA)·H_2O. The equivalent ratio between the solubilities of (R-APE)(R-MA) and (S-APE)(R-MA) in water-free ethyl acetate is *ca.* 2. This may explain why the resolution cannot be achieved in water-free ethyl acetate.

The analysis of the crystal structures of (R-APE)(R-MA)·H_2O and (S-APE)(R-MA) showed that the cations and anions adopt different conformations in the two salts. As described previously the two diastereoisomeric salts display significant variations in their interactions through hydrogen bonding. In the more soluble salt the number of cation–anion interionic interactions is smaller than in the less soluble salt. As the interactions between the water molecule and the ions appear to be essential for the crystal packing the qustion emerges: why does the more soluble (S-APE)(R-MA) salt not have similar interactions and crystallize as a hydrate? Visualizing the packing diagram in Fig. 3 with (R)-2-hydroxy-1-phenylethylammonium ions replaced with cations of opposite configuration it is obvious that this arrangement would lead to less favourable non-bonded interactions, which could explain why (S-APE)(R-MA) does not form an hydrate.

Another question that arises is whether the saturated solution of the unsolvated (R-APE)(R-MA) salt is spontaneously transformed to the solvated (R-APE)(R-MA)·H_2O salt in aqueous ethyl acetate. We assume that the solutions behave ideally and that the activities of the ions can be substituted with their concentrations expressed in mol kg^{-1} solvent. Consequently the $\Delta G^{\ominus}$ values for the four reactions listed in Scheme 1 can be calculated as $\Delta G^{\ominus} = -RT\ln(m/m^{\ominus})^2$.

$$(R\text{-APE})(R\text{-MA})\cdot(\text{Cr}) \longrightarrow R\text{-APE}^+(\text{ea}) + R\text{-MA}(\text{ea}) \qquad \Delta G_1^{\ominus} = 27.1\ \text{kJ mol}^{-1} \quad (1)$$

$$(R\text{-APE})(R\text{-MA})\cdot(\text{H}_2\text{O})(\text{Cr}) \longrightarrow R\text{-APE}^+(\text{ew}) + R\text{-MA}^-(\text{ew}) + \text{H}_2\text{O}(\text{ew}) \qquad \Delta G_2^{\ominus} = 22.3\ \text{kJ mol}^{-1} \quad (2)$$

$$(S\text{-APE})(R\text{-MA})(\text{Cr}) \longrightarrow S\text{-APE}^+(\text{ea}) + R\text{-MA}^-(\text{ea}) \qquad \Delta G_3^{\ominus} = 23.9\ \text{kJ mol}^{-1} \quad (3)$$

$$(S\text{-APE})(R\text{-MA})(\text{Cr}) \longrightarrow S\text{-APE}^+(\text{ew}) + R\text{-MA}^-(\text{ew}) \qquad \Delta G_4^{\ominus} = 15.7\ \text{kJ mol}^{-1} \quad (4)$$

Eqn. (1) − (2) − (3) + (4) gives:

$$(R\text{-APE})(R\text{-MA})(\text{Cr}) + \text{H}_2\text{O}(\text{ew}) + R\text{-APE}^+(\text{ew}) + S\text{-APE}^+(\text{ea}) \longrightarrow (R\text{-APE})(R\text{-MA})\cdot\text{H}_2\text{O}(\text{Cr}) + S\text{-APE}^+(\text{ew}) + R\text{-APE}^+(\text{ea})$$

Scheme 1

Furthermore the solutions are so dilute that the standard chemical potentials will be identical for the two enantiomers of the 2-amino-2-phenylethanol cation in both solvents, *e.g.* $\mu^{\ominus}(R\text{-APE}^+) = \mu^{\ominus}(S\text{-APE}^+)$.

As shown in the Scheme 1 $\Delta G^{\ominus}$ for the reaction (R-APE)(R-MA) + H_2O(ew) ⟶ (R-APE)(R-MA)·H_2O can be calculated, as $\Delta G^{\ominus} = \Delta G_1^{\ominus} - \Delta G_2^{\ominus} - \Delta G_3^{\ominus} + \Delta G_4^{\ominus} = -3.4$ kJ mol^{-1} which shows that the water-free diastereoisomeric salt will be converted into the hydrate in aqueous ethyl acetate.

Acknowledgements

This research was supported through grants from the Danish Natural Science Research Council and The Danish Research Academy (Dávid Kozma's stay). We thank Mr. Flemming Hansen for help with the experimental crystallographic work and Dr. G. Pokol and Katalin Marthi for performing the DSC measurements.

References

1 S. Larsen, M. Ács and D. Kozma, in preparation.
2 G. M. Sheldrick, *Acta Crystallogr., Sect. A*, 1990, **46**, 467.
3 D. Rogers, *Acta Crystallogr., Sect. A*, 1983, **39**, 876.
4 *Structure Determination Package*, Enraf-Nonius, Delft, 1985, The Netherlands.
5 *International Tables of X-ray Crystallography*, Kynoch, Birmingham, 1974, vol. 4, Table 2.
6 *Cambridge Structural Database*, Ver. 5 (1993) University Chemical Laboratory, Lensfield Road, Cambridge, UK.
7 S. Müller, R. Keese, P. Engel and G. Snatzke, *J. Chem. Soc., Chem. Commun.*, 1986, 297.
8 D.-J. Back, S. B. Daniels, P. E. Reed and J. A. Katzenellenbogen, *J. Org. Chem.*, 1989, **54**, 3963.
9 S. Larsen, D. Kozma and M. Ács, *Acta Chem. Scand.* in press.
10 S. Larsen and H. Lopez de Diego, *Acta Crystallogr., Sect. B*, 1993, **49**, 310.

Paper 3/06033K
Received 11*th October* 1993
Accepted 27*th January* 1994